Minimizing Emission for Timely Truck Transportation with Adaptive Fuel Injection

Runzhi Zhou
Case Western Reserve Univ.

Qingyu Liu
Electrical and Computer Engineering
Virginia Tech

Wenjie Xu
Information Engineering
The Chinese Univ. of Hong Kong

Minghua Chen
School of Data Science
City University of Hong Kong

Haibo Zeng
Electrical and Computer Engineering
Virginia Tech

ABSTRACT

We consider the problem of optimizing truck operations, where heavy-duty trucks haul freights that requires timely delivery. The trucks are equipped with engines that intelligently switches among multiple fuel injection strategies for efficient emission profiles. Our objective is to minimize the emission, by optimizing both routing and speed planning while accommodating that modern combustion engines come with multiple control strategies switching at runtime based on the engine speed. Besides the combinatorial nature of simultaneous routing and speed planning that already makes the problem NP-complete, the problem also face the unique challenge that the emission is non-continuous, non-convex with respect to the vehicle speed. We identify a special structure in the problem to provide an analytical solution for the optimal speed profile, and then develop an efficient heuristic for both path planning and speed planning to deal with problems on the scale of national highway systems. We perform simulation on the US highway system, and demonstrate that our approach reduces on average 18% emission compared to the baseline with a single control strategy. Compared to the fastest path approach that is adopted in common practice, our scheme reduces 72% emission on average.

CCS CONCEPTS

• **Mathematics of computing → Paths and connectivity problems**; • **Applied computing → Transportation**.

KEYWORDS

Energy-efficient transportation, timely transportation, engine fuel injection strategy, emission

Figure 1: NOx emission model for different injection strategies [6], and the model corresponding to the code in Figure 2 (shown in thick black line).

1 INTRODUCTION

The trucking industry is vital to the economy. In 2018, trucks hauled 11.49 billion tons of freight in the United States (US), or 71.4% of the total tonnage. It generated $796.7 billion in revenue, nearly a $100 billion increase from the previous year ($700.1 billion in 2017) [4]. It would rank 18th in the world if measured against the GDPs of countries. This trend will likely continue, as the global freight activity is predicted to increase by a factor of 2.4 by 2050 [19].

Meanwhile, heavy duty vehicles are a major source of emissions including Carbon Dioxide (CO_2), Nitrogen Oxides (NOx), and fine particle matter (PM 2.5), thus controlling their exhaust emissions is critical for cleaner environment. Although heavy duty trucks only account for 4% of the total vehicle population, they produce more than one-third of the CO_2 (the primary greenhouse gas causing global warming) emitted in the transportation sector around the world [19]. In US, heavy duty trucks emit about 16-18% of NOx, a pollutant linked to heart and lung disease [11]. In California, one of the most polluted areas in US, heavy duty trucks contribute to over 70% of the NOx emissions from on-road vehicles [10].

A recent effort to reduce the emissions in the transportation sector is the introduction of multiple injection strategies for internal combustion engines, which also improves fuel economy and

```
#define ω₁ 1000
#define ω₂ 2000
#define ω₃ 4000
#define ω₄ 6000

task Engine_control_task {
    ω = read_engine_speed();
    f1();
    if (ω ≤ ω₁)    f2();
    if (ω ≤ ω₂)    f3();
    if (ω ≤ ω₃)    f4();
    if (ω ≤ ω₄)    f5();
}
```

Figure 2: Typical engine control software that switches strategies with the engine speed. [9].

Table 1: Comparison of our work and existing studies on optimizing timely truck operations.

Studied Problem	Design Space		Deadline Constraint	Cost	Cost Model
	Path Planning	Speed Planning			
RSP [14, 21, 25]	✓	✗	✓	Any	Constant
PASO [12, 13] [23, 24, 37]	✓	✓	✓	Fuel	Convex, twice-differentiable
Other, e.g., [15]	✗	✓	✗	Fuel	Any function
Other, e.g., [7]	✓	✗	✗	Fuel	Constant
This work	✓	✓	✓	Emission	Non-convex

reduces combustion noise [17]. Specifically, the engine control system determines the timing and amount of fuel injected in the engine, triggered at predefined rotation angles of the engine crankshaft. In each engine revolution, the engine control system determines the timing and amount of fuel for a number of possible injections: (i) the main injection which provides the bulk of the fuel; (ii) several optional injections (called pilot injections or pre-injections) before the main injection to heat the combustion chamber and ensure a more uniform fuel-air mixture; (ii) one or two optional injections (called post-injections) after the main injection to burn the residual and decrease the amount of pollutants. Figure 1 illustrates the model for the emission of NOx as a function of the engine speed for different injection strategies [6], where the curve for each strategy is approximated with an exponential function that is convex in the engine speed range. In addition, these functions are monotonically decreasing with the number of injections: for any engine speed, the higher the number of injections, the lower the emission is.

However, multiple injections come with the cost of higher computational load. At high engine speeds, the time interval for one engine revolution is small which may not allow sophisticated control strategies (and multiple injections). Hence, engine control systems are designed to be *self-adaptive* in that they switch to simplified control strategies (such as single-injection) at high engine speeds [9]. Figure 2 shows the typical engine control software that is realized as a sequence of conditional `if` statements [6, 9]. The control strategy at a speed higher than ω_4 (i.e., $\omega > \omega_4$) only executes function `f1()` for single-injection, but multiple functions (`f1()`–`f5()`) for quintuple-injection at ω_1. This in general makes the cost model discontinuous at the switching speeds (thus non-convex). As an example, the overall NOx emission model corresponding to the code in Figure 2 is plotted as a thick black line in Figure 1.

We consider a common truck operation scenario where a long-haul truck drives across a national highway. Our objective is to select the path and speed profile of the truck, to minimize the total emission subject to a deadline constraint. Timely transportation is a common requirement in the trucking industry, due to three reasons [12]: (i) the nature of the goods (such as fresh food) [5]; (ii) service-level agreements to guarantee delivery delay such as those in Amazon[1], uShip[2] and Uber Freight[3]; and (iii) ease of scheduling and operation in the logistics [26]. For instance, mobile applications

like uShip and Uber Freight collect freight transportation requests for truck operators, which are often associated with pickup and delivery time requirements.

Although our approach is applicable to any cost function that satisfies the assumptions in Section 3, we focus on minimizing the emission since this is the main benefit of multiple injection strategies in modern internal combustion engines. Our design space includes path planning and speed planning as in several previous studies [12, 13, 23, 24, 37]. However, the consideration of adaptive engine control strategies makes the problem uniquely challenging as the overall emission is a non-continuous, non-convex function with respect to the speed, due to the switching among these control strategies at runtime.

Table 1 summarizes the comparison between our work and related studies on optimizing truck operations, and the details will be presented later in Section 2. In conclusion, we are the first to study the problem of optimizing the operation of a long-haul heavy truck subject to a deadline constraint, where the engine is equipped with multiple injection strategies. Solving our problem requires to simultaneously optimize path planning and speed planning while dealing with the unique challenge that the cost function is non-convex. We make the following specific **contributions** in this paper.

▷ We prove that our problem is NP-hard. We show that dynamically switching among multiple engine control strategies makes the emission rate function non-continuous and non-convex, hence imposing a unique challenge compared to existing studies which all deal with convex cost functions.

▷ We explore the structure of the problem to derive an analytical solution for the optimal speed profile. We further develop a fast heuristic for both path planning and speed planning.

▷ We use the US highway system to demonstrate that our scheme reduces on average 18% emission compared to the baseline with a single control strategy, and saves 72% emission on average compared to the fastest path approach.

2 RELATED WORK

Restricted Shortest Path (RSP): RSP requires to find a path such that the total cost is minimized while the path travel time is within a deadline constraint. RSP is shown to be NP-hard [14], for which heuristic algorithms [21] and fully polynomial time approximation schemes (FPTAS) [14, 25] are designed. RSP only involves path planning and assumes fixed speeds. Moreover, RSP considers a fixed cost for passing an edge. Therefore, existing results on RSP cannot be directly applied to the setting in this paper, where the

---

[1]Place an Order with Guaranteed Delivery, Amazon, http://amazon.com
[2]uShip, https://www.uship.com/
[3]Uber Freight, https://freight.uber.com/

challenging design space of speed planning with non-convex cost function has to be efficiently handled.

PAth selection and Speed Optimization (PASO) and its extensions: PASO [12, 13] generalizes RSP with speed planning taken into account. Deng *et al.* [12, 13] develop both an FPTAS and a heuristic for PASO. Liu *et al.* [23, 24] extend PASO to a multi-task setting, to fulfill multiple transportation tasks under task pickup and delivery time window constraints. Xu *et al.* [37] consider dynamic traffic conditions such that it might be beneficial to wait for benign traffic conditions (i.e., opportunistic driving). However, all these studies assume the fuel consumption model is convex, and cannot be easily generalized to the problem of emission minimization, where the cost function is non-convex due to multiple injection strategies.

Other studies: Hellström *et al.* [15] consider a weighted average of travel time and fuel consumption as the cost function, and use look-ahead information such as estimated road grade [29] to control the truck's speed trajectory under a given path. Boriboonsomsin *et al.* [7] present an eco-routing navigation system that determines the most fuel-economic path. Scora *et al.* [30] analyze the tradeoff between the amount of fuel savings and the added travel time relative to the fastest path. Both studies [7, 30] assume fixed road driving speeds and hence no speed planning is involved. Alam *et al.* [2] observe that improved fuel-efficiency can be obtained by maintaining the platoon of trucks throughout a hill, motivating subsequent studies, e.g., [1, 3], which focus on developing control strategies for truck platooning to save fuel.

Meanwhile, emission control has been a continuous effort from both the industry and the regulatory authorities, see a recent review in [20]. In particular, heavy-duty engines are improving at a much slower pace than light-duty ones [20]. However, these studies all focus on the optimization of design and operation of various parts in the engine (e.g., fuel system and injection strategy [6, 22, 27, 31], exhaust after-treatment system [18]), and *do not consider the planning of path and/or speed profile*. For example, Biondi *et al.* [6] present methods to optimize the switching speeds of multiple injection strategies at design time against standard driving cycles (i.e., with fixed path and speed profile), while Peng *et al.* [27] propose to adjust the switching speeds at runtime using predicted driving cycle.

Overall to our best knowledge, we are the first to study the problem of minimizing emission for a long-haul heavy truck equipped with multiple engine control strategies. Compared to existing studies that also simultaneously optimize path planning and speed planning under a deadline constraint [12, 13, 23, 24, 37], the consideration of switching among multiple injection strategies makes our problem uniquely challenging, since the emission rate function is non-continuous, non-convex, as opposed to a convex cost function for fuel-rate in [12, 13, 23, 24, 37].

3 PROBLEM DEFINITION

We model a national highway network as a directed graph $G \triangleq (V, E)$ where an edge $e \in E$ represents a road segment, and a node $v \in V$ represents a point of junction for multiple road segments. The environmental conditions of a road segment that can impact the emission rate of a truck, e.g., grade and surface resistance are assumed to be homogeneous (otherwise it is broken into multiple appropriate segments). We consider the scenario where a truck travels from a source $o \in V$ to a destination $d \in V$ across the highway network G within a hard deadline requirement T.

We denote the distance of an edge $e \in E$ as $D^e > 0$. We let $f^e(r)$ be the cost function such as the emission rate (the emission in a time unit) for the truck to pass e following a constant speed of r. We use vehicle speed instead of engine speed in the cost model, since the vehicle speed is proportional to the engine speed in a vehicle [28, Section 1.6]. We assume $f^e(r)$ is an n piece-wise convex, staircase-shaped function (see, e.g., Figure 1), where n is the number of engine control strategies. More specifically, $f^e(r)$ is defined as

$$f^e(r) = f_i^e(r) \quad \text{if } r \in (s_{i-1}, s_i] \tag{1}$$

where $s_0^e = (r_l^e)^-$ and r_l^e is the minimum speed on edge e, $s_n^e = r_u^e$ is the maximum speed. s_i^e is the switching speed from strategy i to $i + 1$, and $s_i^e < s_j^e, \forall i < j$. Hence, $(s_{i-1}^e, s_i^e]$ defines the speed interval that adopts the strategy i and thus follows the cost model f_i^e. We assume that $f^e(r)$ satisfy the following two assumptions:

- **piece-wise convex**: each function f_i^e is convex over the interval $[r_l^e, r_u^e]$;
- **staircase-shaped**: they satisfy that

$$\forall i < j \in [n], \forall r \in [r_l^e, r_u^e], \quad f_i^e(r) < f_j^e(r) \tag{2}$$

where $[n]$ denotes the set of positive integers no larger than n.

We remark that the above assumptions on the cost model is realistic for a number of metrics related to the efficient and environment-friendly truck operations. For example, the fuel-rate is described as a polynomial function of the vehicle speed, verified with both a theoretical study and experimental data [13]. The emitted CO_2 is approximately proportional to the amount of fuel (e.g., about 10.18kg per gallon of diesel, or 8.887kg per gallon of gasoline) [33], hence it follows the same characteristics as the fuel-rate function. Similarly, the NOx emission is approximated with an exponential function that remains convex in the engine speed range (hence the vehicle speed as well) based on extensive simulation data [6]. For the second assumption (Equation (2)), this is based on the rationale that a more complex fuel injection strategy only makes sense if it provides some benefit such as reduced emission, but its complexity makes it only feasible at lower speeds [6]. In the rest of the paper we focus on emission, but the approach is generally applicable to any cost function that satisfies the above assumptions.

With the emission rate function $f^e(r)$ for each edge e, we can define its emission function $c^e(t)$ that gives the total emission for the truck to traverse e with a travel time of t. Later in Corollary 7, we show how to calculate $c^e(t)$ given $f^e(r)$ and t. With $c^e(t)$, the efficient timely truck transportation problem is formulated as

$$\min_{x \in \mathcal{X}, t \in \mathcal{T}} \sum_{e \in E} x^e \cdot c^e(t^e) \tag{3a}$$

$$\text{s.t.} \sum_{e \in E} x^e \cdot t^e \leq T, \tag{3b}$$

where $\mathcal{X}$ defines a simple path from o to d

$$\mathcal{X} \triangleq \{x : x^e \in \{0, 1\}, \forall e \in E, \text{ and}$$

$$\sum_{e \in \text{out}(v)} x^e - \sum_{e \in \text{in}(v)} x^e = 1_{\{v=o\}} - 1_{\{v=d\}}, \forall v \in V\}.$$

Here $1_{\{\cdot\}}$ is the indicator function, $\text{in}(v) \triangleq \{(u, v) : (u, v) \in E\}$ is the set of incoming edges of node v, $\text{out}(v) \triangleq \{(v, u) : (v, u) \in E\}$

is the set of outgoing edges of node v. The set $\mathcal{T}$ captures the speed limits of all roads, which is defined as

$$\mathcal{T} \triangleq \{t : t_l^e \leq t^e \leq t_u^e, \forall e \in E\},$$

where $t_l^e = \frac{D^e}{r_u^e}$ and $t_u^e = \frac{D^e}{r_l^e}$ are the minimum and maximum travel times of traversing the edge e, respectively. Overall, we need to find a routing and speed planning solution (i.e., a path from o to d, with driving speed assigned to each edge on the path) such that the total emission is minimized, under the constraint that the total travel time is no greater than T.

THEOREM 1. *The problem defined in Equation (3) is NP-complete.*

PROOF. This directly follows the fact that the NP-complete problem PASO is a special case of our problem, where PASO only contains one control strategy (and $n = 1$). □

4 SPEED PLANNING

In this section, we tackle the issue of speed planning: given an emission rate function $f^e(r)$ for an edge e, how to derive its emission function $c^e(t)$ for any given $t \in [t_l^e, t_u^e]$. For ease of presentation, *we omit the superscript ^{e} from the notations in the rest of the section, e.g., $f^e(r)$ is simplified as $f(r)$.*

In related studies [12, 13, 23, 24, 37] where each edge has a convex cost function, it is proven that the optimal solution is to drive at a constant speed to pass the edge (see e.g., Lemma 1 of [13]). In sharp contrast, in our problem the cost function of each edge is non-continuous containing multiple pieces, hence is non-convex [35] and even can be shown to be non-quasi-convex. We highlight with Example 4.1 below that driving at a constant speed does not minimize the cost of passing the edge. Despite that the cost function is non-convex, we are able to provide a convex programming formulation (Section 4.1) and even an analytical solution (Section 4.2) for speed planning, by carefully leveraging its special structures.

Example 4.1. Let us consider the following emission rate function

$$f(r) = \begin{cases} (r-30)^2/100 + 1 & \text{if } 30 \leq r \leq 50, \\ (r-50)^2/100 + 10 & \text{if } 50 < r \leq 60 \end{cases}$$

It is clear that the above function is a piece-wise convex function that satisfies our assumptions. We further assume the length of the edge is 110, and the total travel time for traversing this edge is 2.

(i) By following a constant speed of $110/2 = 55$, the emission is

$$2 \cdot f(55) = 2(25/100 + 10) = 20.5$$

(ii) In comparison, consider another solution where we first drive at a speed of 40 for time 0.5, and then drive at a speed of 60 for time 1.5. This solution is feasible since it traverses the edge (with a length of 110) by a total travel time of 2. The incurred emission is

$$0.5 \cdot f(40) + 1.5 \cdot f(60) = 0.5(100/100 + 1) + 1.5(100/100 + 10) = 17.5$$

Obviously driving at a constant speed 55 incurs a larger emission than the solution (ii), hence the former is not necessarily optimal.

4.1 A Convex Programming Formulation

Although driving at a constant speed is not necessarily optimal, we first observe a similar lemma to Lemma 1 of [13]: for each piece $f_i(r)$, it is always optimal to just choose some constant speed r_i in its speed range $(s_{i-1}, s_i]$.

LEMMA 2. *If the total travel time t_i following the speed in the range $(s_{i-1}, s_i]$ of the i-th piece $f_i(r)$ is given, then the optimal speed profile is to maintain some constant speed r_i for the whole duration t_i.*

PROOF. It is proven similarly to [13, Lemma 1], by applying the continuous Jensen's inequality to the convex function $f_i(r)$. □

With Lemma 2, we now formulate the problem of optimizing the speed profile to pass an edge, where the length of the edge is D, and the total travel time is given as t. Let r_i and t_i be the selected speed and travel time for the i-th piece, respectively. We introduce the auxiliary variable $d_i = r_i \cdot t_i$ to denote the driving distance for the i-th piece, and formulate the problem as

$$c(t) = \min_{t_i \geq 0, d_i \geq 0, \forall i \in [n]} \sum_{i \in [n]} t_i \cdot f_i\left(\frac{d_i}{t_i}\right) \tag{4a}$$

$$\text{s.t.} \quad \sum_{i \in [n]} t_i = t, \quad \sum_{i \in [n]} d_i = D \tag{4b}$$

$$s_{i-1} t_i \leq d_i \leq s_i t_i, \forall i \in [n] \tag{4c}$$

The objective is the total emission on the road segment. We require the total driving distance be equal to the length D of the road segment, and the total travel time be t. We also require the driving speed $\frac{d_i}{t_i}$ be within the corresponding speed range.

This formulation avoids r_i but uses d_i and t_i, the driving time and driving distance corresponding to the i-th piece, which makes it particularly easy to see that it is a convex program.

THEOREM 3. *The speed planning problem in (4) is a convex optimization problem.*

PROOF. Obviously the constraints are all linear. The objective function is convex with respect to each d_i and t_i, since each summand $t_i \cdot f_i\left(\frac{d_i}{t_i}\right)$ is the perspective of the convex function f_i, thus it must be convex as well [8]. □

Theorem 3 indicates that the problem of speed planning alone can be efficiently solved as a standard convex program. However, its proof only leverages the assumption that each piece in the emission rate function is convex. We further provide an analytical solution to (4), by additionally utilizing the assumption in Equation (2).

4.2 An Analytical Solution

We now rewrite problem (4) in the following equivalent form

$$f^*(\bar{r}) = \min_{\beta_i \geq 0, r_i \geq 0, \forall i \in [n]} \sum_{i \in [n]} \beta_i \cdot f_i(r_i)$$

$$\text{s.t.} \quad \sum_{i \in [n]} \beta_i = 1, \quad \sum_{i \in [n]} \beta_i \cdot r_i = \bar{r} \tag{5}$$

$$r_i \in (s_{i-1}, s_i], \ \forall i \in [n]$$

where $\beta_i = \frac{t_i}{t}$, and $\bar{r} = \frac{D}{t}$. Essentially, problem (5) is to find a set of speeds, one r_i for each piece i, such that their convex combination is equal to the average speed $\bar{r} = \frac{D}{t}$ over the edge, and

the weighted average of the emission rate is minimized (denoted as $f^*(\bar{r})$). Obviously $c(t) = tf^*(D/t)$, that is, $c(t)$ is the perspective of the function f^* [8].

For an arbitrary emission rate function $f(r)$ containing $n > 1$ pieces, we now show how the corresponding problem (5) can be decoupled into two subproblems, each of which concerning the minimization of the emission rate in a convex combination. We first define a new function $\hat{f}(r)$ containing $n-1$ pieces, which is the same as $f(r)$ except that the last speed interval $(s_{n-1}, s_n]$ uses the cost function of the $(n-1)$-th piece f_{n-1}.

$$\hat{f}(r) = \begin{cases} f(r) & \text{if } r \le s_{n-2}, \\ f_{n-1}(r) & \text{if } r > s_{n-2} \end{cases} \tag{6}$$

We define the average speed $\hat{r}$ for the first $n-1$ pieces as $\hat{r} \sum_{i \in [n-1]} \beta_i = \sum_{i \in [n-1]} \beta_i r_i$. The following optimization problem minimizes the emission rate with the cost function $\hat{f}$ and a given average speed $\hat{r} \in (s_0, s_n]$:

$$\hat{f}^*(\hat{r}) = \min_{\alpha_i \ge 0, r_i, \forall i \in [n-1]} \sum_{i \in [n-1]} \alpha_i \cdot f_i(r_i)$$
$$\text{s.t.} \sum_{i \in [n-1]} \alpha_i = 1, \sum_{i \in [n-1]} \alpha_i \cdot r_i = \hat{r} \tag{7}$$
$$r_i \in (s_{i-1}, s_i], \ \forall i \in [n-2]$$
$$r_{n-1} \in (s_{n-2}, s_n]$$

where α_i is the normalized coefficient of β_i, i.e., $\alpha_i \sum_{i \in [n-1]} \beta_i = \beta_i$.

Now we define the optimization of the convex combination between $\hat{f}^*$ and f_n

$$f^*(\bar{r}) = \min_{\beta_n, r_n, \hat{r}} (1-\beta_n)\hat{f}^*(\hat{r}) + \beta_n f_n(r_n)$$
$$\text{s.t.} \quad (1-\beta_n)\hat{r} + \beta_n r_n = \bar{r} \tag{8}$$
$$0 \le \beta_n \le 1, \hat{r} \in (s_0, s_{n-1}], r_n \in (s_{n-1}, s_n]$$

Problem (5) now can be decomposed into two subproblems that are solved separately. (i) Given any $\hat{r}$, solve the problem (7) to derive the optimal solution $\hat{f}(\hat{r})$; (ii) Given any r, find the optimal convex combination to problem (8). Note that in (8) the constraint $\hat{r} \le s_{n-1}$ (instead of $\hat{r} \le s_n$) is derived by the fact that $\hat{r}$ is a convex combination of $r_1, \dots r_{n-1}$. This decomposition is based on the observation that the objective function in (5) is a convex combination of the contribution from f_n and those of all the other pieces f_i, hence can be optimized separately. Specifically,

$$f^*(\bar{r}) = \min_{\beta_i, r_i, \forall i \in [n]} \sum_{i \in [n]} \beta_i f_i(r_i)$$
$$= \min_{\beta_i, r_i, \forall i \in [n]} \sum_{i \in [n]} \left\{ \beta_n f_n(r_n) + (1-\beta_n) \sum_{i \in [n-1]} \alpha_i f_i(r_i) \right\}$$
$$\overset{(E1)}{=} \min_{\beta_n, r_n, \hat{r}} \left\{ \beta_n f_n(r_n) + (1-\beta_n) \min_{\hat{r}, \alpha_i, r_i, \forall i \in [n-1]} \sum_{i \in [n-1]} \alpha_i f_i(r_i) \right\}$$
$$= \min_{\beta_n, r_n, \hat{r}} \{ \beta_n f_n(r_n) + (1-\beta_n)\hat{f}^*(\hat{r}) \}$$

Here the equality $(E1)$ is due to that (a) given $\hat{r}$, β_n becomes independent from $r_1, \dots r_{n-1}$ and $\alpha_1, \dots \alpha_{n-1}$; and (b) $\sum_{i \in [n-1]} \alpha_i f_i(r_i)$ is independent from β_n and r_n.
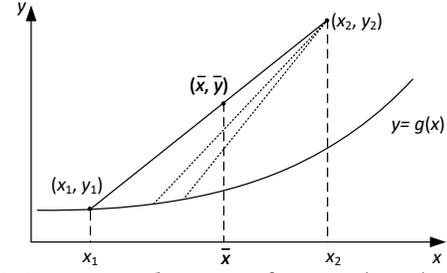
Figure 3: Convex combination of a point (x_1, y_1) on a convex curve $y = g(x)$ and a point (x_2, y_2) that is above the curve and to the right of x_1.
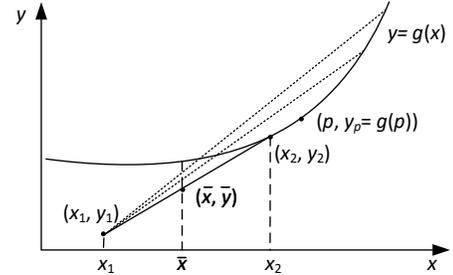
Figure 4: Convex combination of a point (x_2, y_2) on a convex curve $y = g(x)$ and a point (x_1, y_1) that is below the curve and to the left of x_1. (p, y_p) is the generalized point of tangency from (x_1, y_1) to the curve $y = g(x)$ with $p > x_1$.

We note that essentially problem (8) is to find a point $(\hat{r}, \hat{f}(\hat{r}))$ on the curve $\hat{f}$ and another one $(r_n, f_n(r_n))$ on the curve f_n, such that the speed of their convex combination is $\bar{r}$, and the cost is minimized. Like $f_n(\cdot)$, $\hat{f}$ is shown to be convex (Theorem 6). We first introduce two lemmas that are useful for solving (8).

LEMMA 4. *Consider a convex function $g(x)$, a point (x_2, y_2) above the curve of $y = g(x)$, i.e., $y_2 > g(x_2)$, and $\bar{x} \le x_2$. For every $x_1 < \bar{x}$, let $(\bar{x}, \bar{y})$ be the convex combination of $(x_1, y_1 = g(x_1))$ and (x_2, y_2) such that the weighted average of x_1 and x_2 is $\bar{x}$, that is, it defines*

$$\bar{y} = \{(1-\beta)y_1 + \beta y_2 : 0 \le \beta \le 1, (1-\beta)x_1 + \beta x_2 = \bar{x}\} \tag{9}$$

Then for every fixed $\bar{x}$ and $x_2 \ge \bar{x}$, $\bar{y}$ is monotonically non-increasing with x_1 for $x_1 < \bar{x}$. In addition, $\bar{y} \ge g(\bar{x})$.

We leave the proof in Appendix 8.1. Figure 3 provides the intuition behind Lemma 4: Equation (9) enforces that $(\bar{x}, \bar{y})$ is the intersection between two lines: the vertical line $x = \bar{x}$ and the line connecting $(x_1, y_1 = g(x_1))$ and (x_2, y_2). As in the figure, when x_1 is moving to the right (until $\bar{x}$) along the convex curve $y = g(x)$, its y intercept with the vertical line $x = \bar{x}$ is always non-increasing, i.e., $\bar{y}$ is monotonically non-increasing with the increase of x_1.

Lemma 4 is about the convex combination for a point on the convex curve and another one that is right to the point and above the curve. The following lemma discusses a different scenario, on the convex combination of a point on the convex curve and another one that is left to the point and below the curve.

LEMMA 5. *Consider a convex function $g(x)$ and a fixed point (x_1, y_1) that is below the curve of $y = g(x)$, i.e., it satisfies $y_1 < g(x_1)$.*

Define $(p, y_p = g(p))$ as the **generalized right** point of tangency from (x_1, y_1) to its right hand side of the curve $y = g(x)$, i.e., $p > x_1$ satisfies the following equation

$$\partial_- g(p) \le \frac{g(p) - y_1}{p - x_1} \le \partial_+ g(p) \tag{10}$$

where $\partial_- g(p)$ and $\partial_+ g(p)$ are the left and right derivatives of g at p.

Given $\bar{x} > x_1$, for every $x_2 \ge \bar{x}$, let $(\bar{x}, \bar{y})$ be the convex combination between (x_1, y_1) and $(x_2, y_2 = g(x_2))$ such that the weighted average of x_1 and x_2 is $\bar{x}$, that is, it defines

$$\bar{y} = \{(1 - \beta)y_1 + \beta y_2 : 0 \le \beta \le 1, (1 - \beta)x_1 + \beta x_2 = \bar{x}\} \tag{11}$$

Then $\bar{y}$ has the following properties:

- If $\bar{x} \le p$, then $\bar{y}$ is monotonically non-increasing with x_2 until p, and monotonically non-decreasing with x_2 afterwards. In addition, $\forall \bar{x} \le x_2 \le p, \bar{y} \le g(\bar{x})$.
- If $\bar{x} \ge p$, then $\bar{y}$ is monotonically non-decreasing with x_2. In addition, $\forall x_2 \ge \bar{x}, \bar{y} \ge g(\bar{x})$.

Note that for a convex function, the **generalized** point of tangency in Equation (10) is well defined, since a convex function is semi-differentiable thus allows left and right derivatives [36], and these derivatives are always non-decreasing [35].

Similarly, we provide the proof in Appendix 8.2, while using Figure 4 to provide an illustrative explanation for the case of $\bar{x} \le p$.

We now present the main result of this section, that is applicable to any piece-wise convex, staircase-shaped cost functions. The intuition is that the optimal solution to the subproblem (7) gives a convex function $\hat{f}^*$, and the optimal solution to the subproblem (8) can leverage Lemmas 4 and 5 to quickly find an analytical solution.

THEOREM 6. *Given the total travel time t and hence the average speed $\bar{r} = D/t$ to pass an edge, assume $\bar{r} \in (s_{i-1}, s_i]$ for some $i \in [n]$. In case that $i > 1$, let $(p_i, f_i(p_i))$ be the generalized right point of tangency from $(s_{i-1}, f_{i-1}(s_{i-1}))$ to the curve f_i (hence $p_i > s_{i-1}$). Then the optimal solution and minimized cost to problem (5) are*

$$(i) \; if \, (i = 1) : \begin{cases} r_1 = \bar{r}, \beta_1 = 1 \\ \beta_j = 0, \forall j \ne 1 \\ f^*(\bar{r}) = f_1(\bar{r}) \end{cases}$$

$$(ii) \; if \, (i > 1 \wedge \bar{r} \le p_i) : \begin{cases} r_{i-1} = s_{i-1}, r_i = \min\{p_i, s_i\} \\ \beta_{i-1} = \frac{r_i - \bar{r}}{r_i - r_{i-1}}, \beta_i = \frac{\bar{r} - r_{i-1}}{r_i - r_{i-1}} \\ \beta_j = 0, \forall j \ne i - 1 \wedge j \ne i \\ f^*(\bar{r}) = \frac{r_i - \bar{r}}{r_i - r_{i-1}} f_{i-1}(r_{i-1}) + \frac{\bar{r} - r_{i-1}}{r_i - r_{i-1}} f_i(r_i) \end{cases}$$

$$(iii) \; if \, (i > 1 \wedge \bar{r} \ge p_i) : \begin{cases} r_i = \bar{r}, \beta_i = 1 \\ \beta_j = 0, \forall j \ne i \\ f^*(\bar{r}) = f_i(\bar{r}) \end{cases} \tag{12}$$

Furthermore, $f^*(\bar{r})$ is convex over $\bar{r} \in (s_0, s_n]$.

PROOF. See Appendix 8.3. □

COROLLARY 7. *The analytical solution of $c(t)$ can be derived from that of f^* as $c(t) = t \cdot f^*(\bar{r}) = t \cdot f^*(\frac{D}{t})$. Furthermore, $c(t)$ is convex over $t \in [t_l, t_u]$.*

PROOF. This directly follows the fact that $c(t)$ is the perspective of the convex function f^* [35]. □

5 AN EFFICIENT HEURISTIC

With the analytical solution to the speed planning for a given travel time t on an edge e and hence a closed-form formula for $c^e(t)$, we consider the overall problem (3) which now amounts to find a path and assign a travel time to each edge on the path, such that the emission is minimized and the total travel time is no larger than the deadline T. We design an efficient heuristic based on Lagrangian relaxation, and derive a theoretical condition under which our heuristic must output the optimal solution. As in the experiments, for the scale of the US national highway network, our heuristic always quickly finds close-to-optimal solutions.

5.1 Lagrangian Relaxation and Dual Problem

We introduce a Lagrangian dual variable $\lambda \ge 0$, and derive the Lagrangian relaxation for problem (3) as

$$L(x, t, \lambda) \triangleq \sum_{e \in E} x^e \cdot c^e(t^e) + \lambda \cdot (\sum_{e \in E} x^e \cdot t^e - T)$$
$$= \sum_{e \in E} x^e \cdot (c^e(t^e) + \lambda \cdot t^e) - \lambda \cdot T.$$

The corresponding dual function is defined as

$$D(\lambda) \triangleq \min_{x \in X, t \in \mathcal{T}} L(x, t, \lambda).$$

and the dual of the original problem (3) is $\max_{\lambda \ge 0} D(\lambda)$.

Given λ, we have the following observation on $D(\lambda)$ by following its definition above:

$$D(\lambda) = -\lambda T + \min_{x \in X} \left[\min_{t \in \mathcal{T}} \sum_{e \in E} x^e \cdot (c^e(t^e) + \lambda t^e) \right]$$
$$= -\lambda T + \min_{x \in X} \sum_{e \in E} x^e \cdot \min_{t_l^e \le t^e \le t_u^e} (c^e(t^e) + \lambda t^e)$$
$$\stackrel{(a)}{=} -\lambda T + \min_{x \in X} \sum_{e \in E} x^e \cdot [c^e(t^{e*}(\lambda)) + \lambda \cdot t^{e*}(\lambda)]$$
$$\stackrel{(b)}{=} -\lambda T + \min_{x \in X} \sum_{e \in E} x^e \cdot w^e(\lambda)$$
$$\stackrel{(c)}{=} -\lambda T + \sum_{e \in p^*(\lambda)} w^e(\lambda), \tag{13}$$

Here $t^{e*}(\lambda)$ in (a) is defined as

$$t^{e*}(\lambda) \triangleq \arg \min_{t_l^e \le t^e \le t_u^e} (c^e(t^e) + \lambda t^e). \tag{14}$$

i.e., $t^{e*}(\lambda)$ is the optimal travel time that minimizes $c^e(t^e) + \lambda t^e$ for edge $e \in E$, $w^e(\lambda)$ in (b) is the corresponding optimal cost

$$w^e(\lambda) \triangleq c^e(t^{e*}(\lambda)) + \lambda \cdot t^{e*}(\lambda), \tag{15}$$

and $p^*(\lambda)$ in (c) is the resulting minimum-cost path where each edge is associated with an edge cost of $w^e(\lambda)$. Given a value to the dual variable λ, Equation (13) suggests that we can figure out $D(\lambda)$, the value of the dual function, by finding a shortest path with each edge e assigned an edge cost of $w^e(\lambda)$. In the following, we first derive an analytical solution to $t^{e*}(\lambda)$ and hence $w^e(\lambda)$ for each edge $e \in E$, then in Section 5.2 we propose an iterative procedure to find an appropriate value for λ.

In Theorem 6, for each edge $e \in E$ we provide an analytical solution for f^{e*}, from which the function $c^e(t) = t \cdot f^{e*}(D^e/t)$

can easily be derived. Furthermore, Corollary 7 shows that $c^e(t)$ is convex, hence it allows left and right derivatives. The following lemma provides an analytical solution to $t^{e*}(\lambda)$ and hence $w^e(\lambda)$.

LEMMA 8. *In case that* $\partial_+ c^e(t_l^e) \leq -\lambda \leq \partial_- c^e(t_u^e)$, *define* t^* *as any* t *such that* $\partial_- c^e(t) \leq -\lambda \leq \partial_+ c^e(t)$, *which is well-defined since the derivatives of the convex function* $c^e(t)$ *are non-decreasing. Then* $t^{e*}(\lambda)$ *is given as*

$$t^{e*}(\lambda) = \begin{cases} t_l^e, & \text{if } \lambda + \partial_+ c^e(t_l^e) > 0 \\ t^*, & \text{if } \partial_+ c^e(t_l^e) \leq -\lambda \leq \partial_- c^e(t_u^e) \\ t_u^e, & \text{if } \lambda + \partial_- c^e(t_u^e) < 0 \end{cases} \tag{16}$$

PROOF. Observe that $c^e(t) + \lambda t$ is also convex with respect to t. Hence its derivatives are non-decreasing.

If $\lambda + \partial_+ c^e(t_l^e) > 0$, then $c^e(t) + \lambda t$ is non-decreasing for $t \geq t_l^e$, hence its minimum is achieved at the lower bound of t, i.e., t_l^e. If $\lambda + \partial_- c^e(t_u^e) < 0$, then $c^e(t) + \lambda t$ is non-increasing for $t \leq t_u^e$, hence its minimum is achieved at the upper bound of t, i.e., t_u^e.

If $\partial_+ c^e(t_l^e) \leq -\lambda \leq \partial_- c^e(t_u^e)$, then the derivatives of $c^e(t) + \lambda t$ remain to be non-positive for $t < t^*$, and then are always non-positive for $t > t^*$, hence its minimum is achieved at t^*. □

When $\partial_+ c^e(t_l^e) \leq -\lambda \leq \partial_- c^e(t_u^e)$, we can find t^* with a binary search scheme, since the derivatives of the convex function c^e is non-decreasing. The complexity is $O(\log \lceil \frac{t_u^e - t_l^e}{\epsilon_t} \rceil)$ where ϵ_t is the level of error tolerance for t.

5.2 Our Heuristic Algorithm

For a given λ, we define $\delta(\lambda)$ as follows

$$\delta(\lambda) \triangleq \sum_{e \in p^*(\lambda)} t^{e*}(\lambda), \tag{17}$$

which is the total travel time of the minimum-cost path $p^*(\lambda)$ for a given λ. We introduce an important observation on $\delta(\lambda)$ below.

LEMMA 9. $\delta(\lambda)$ *is non-increasing over* $\lambda \in [0, +\infty)$.

PROOF. Refer to [13, Thm. 3], which is still applicable to our problem since it only uses the facts that $t^{e*}(\lambda)$ minimizes $c^e(t) + \lambda t$ and $p^*(\lambda)$ is the minimum-cost path. □

By the Lagrangian dual relaxation, the value of $D(\lambda)$ as calculated in (13) is always a lower bound of the minimized emission to the original problem (3). Hence, we observe that the Lagrangian dual variable λ^* with $\delta(\lambda^*) = T$ defines the optimal solution $\mathcal{P}^*(\lambda^*)$. By Lemma 9, our heuristic suggests to use a binary-search scheme to update λ to approach λ^*, by comparing $\delta(\lambda)$ with T. The details of our heuristic is described in Algorithm 1, where ϵ_λ is the level of error tolerance for λ. λ can be interpreted as a price on the delay, hence $\lambda_{\max}$ can be set as the upper bound on the emission rate.

In the algorithm, whenever we find a λ such that $\delta(\lambda) = T$ (Line 8), it must be the optimal value λ^*. If $\delta(\lambda) > T$ (Line 10), then the deadline constraint is violated, and we set λ as the new lower bound λ_l. Otherwise (Line 12), besides setting λ as the new upper bound λ_u, it can also be used to derive a feasible solution.

We highlight that our heuristic has a strong theoretical performance guarantee, as stated in the following theorem.

Algorithm 1 Our Heuristic Approach

1: **procedure**
2:     Set $\lambda_l = 0$ and $\lambda_u = \lambda_{\max}$
3:     **while** $\lambda_u - \lambda_l > \epsilon_\lambda$ **do**
4:         Set $\lambda = \frac{\lambda_l + \lambda_u}{2}$
5:         Obtain $t^{e*}(\lambda)$ according to Lemma 8 for all $e \in E$
6:         Set $w^e(\lambda)$ according to Equation (15) for all $e \in E$
7:         Get the shortest path $p^*(\lambda)$ from o to d in G
8:         **if** $\delta(\lambda) = T$ **then**
9:             **return** $p^*(\lambda)$ and $\{t^{e*}(\lambda), \forall e \in E\}$
10:       **else if** $\delta(\lambda) > T$ **then**
11:          Set $\lambda_l = \lambda$
12:       **else**
13:          Set $\lambda_u = \lambda, p^* = p^*(\lambda)$, and $\{t^{e*} = t^{e*}(\lambda), \forall e \in E\}$
14:     **return** p^* and $\{t^{e*}, \forall e \in E\}$

THEOREM 10. *If Algorithm 1 returns in Line 9, then the returned solution is optimal to our problem. Otherwise if Algorithm 1 returns in Line 14, the returned solution* $\mathcal{S} = (p^*$ *and* $\{t^{e*}, \forall e \in E\})$ *satisfies the deadline constraint* T *and hence is feasible. Furthermore, it has the following theoretical performance guarantee:*

$$C(\mathcal{S}) - OPT \leq \lambda^\times \cdot (T - \delta(\lambda^\times)), \tag{18}$$

where $C(\mathcal{S})$ *is the total emission of the solution* $\mathcal{S}$, *OPT is the optimal emission of our problem, and* $\lambda^\times$ *is the value of the dual variable corresponding to the returned solution* $\mathcal{S}$.

PROOF. By Equation (13), for a given dual variable λ, the duality gap of our problem is:

$$\text{Duality Gap} = \lambda \cdot (T - \delta(\lambda)), \tag{19}$$

hence the theorem holds. □

We now analyze the complexity of Algorithm 1. The total number of iterations is $O(\log \frac{\lambda_{\max}}{\epsilon_\lambda})$. Within each iteration, the calculation of the optimal $t^{e*}(\lambda)$ and $w^e(\lambda)$ for all edges takes time $O(m \cdot \log \lceil \frac{t_{\max} - t_{\min}}{\epsilon_t} \rceil)$ where m is the number of edges in the highway network, $t_{\max}$ ($t_{\min}$) is the maximum (minimum) travel time among all edges. The shortest path finding step takes time $O(m + k \cdot \log k)$, where k is the number of vertices. Hence, overall Algorithm 1 has a time complexity of $O(\log \frac{\lambda_{\max}}{\epsilon_\lambda} (m \cdot \log \lceil \frac{t_{\max} - t_{\min}}{\epsilon_t} \rceil + m + k \cdot \log k))$.

6 PERFORMANCE EVALUATION

In this section, we present the experimental results on the US national highway system (NHS) consisting of 84504 nodes and 178238 directed edges, which is constructed from the Map-based Educational Tools for Algorithm Learning (METAL) project [32]. Road grade is derived from the elevations of each node provided by the Elevation Point Query Service [34]. The NHS graph is then pre-processed as follows: (i) non-intersection roads with the same grade (we use 0.4% as the span of a grade level) are merged into a single road segment, and (ii) the "eastern" US is divided into 22 regions as shown in Fig. 5, where the node nearest to each region's center is used as the source and destination nodes in the experiments. After pre-processing, the number of nodes is 38213 and the number of
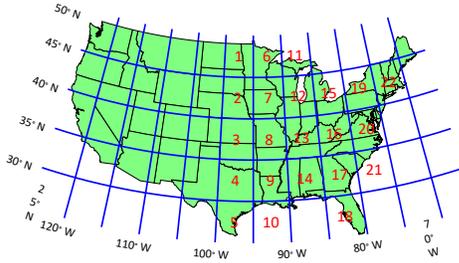
Figure 5: US map (the eastern part is divided into 22 regions).
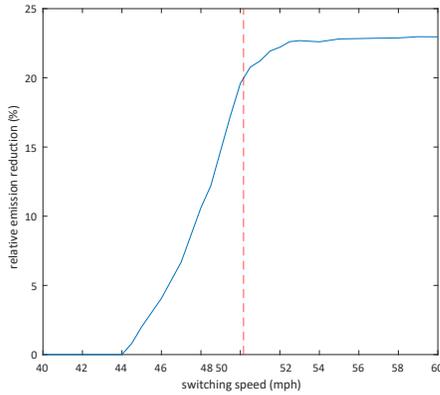
Figure 6: Reduced emission from MFI compared to PASO vs. switching speed. The dashed line denotes the average speed to meet the deadline (24 hours) along the fastest path.

edges (road segments) is 82781. We set the maximum speed r_u^e of a road segment e as the historical average speed, by collecting real-time speed data from HERE map [16] for 2 weeks. The minimum speed r_l^e is manually set to be $r_l^e = \min\{30\text{mph}, r_u^e\}$, where mph (miles per hour) is the unit for speed. The emission model follows that of [6], which considers two fuel injection strategies: single-injection and triple-injection, and the fuel rate function of each strategy is approximated with an exponential function. The overall emission rate function satisfies the two assumptions in Section 3.

We compare three methods in the experiments:

- MFI: our heuristic algorithm with multiple injection strategies, where we set ϵ_λ and ϵ_t to be both 0.01.
- PASO: the baseline approach from [12, 13], which only considers the single injection.
- FAST: the fastest path driving at its maximum speed.

We first use a representative pair $(o, d) = (11, 14)$ of source and destination to demonstrate the benefit of our approach, i.e., the source node o is in region 11, and the destination node d is in region 14. For this pair, the travel time of FAST is about 18.23 hours.

We study how the switching speed affects the amount of emission reduction. We set the deadline to be 24 hours, or about 1.32 times of the travel time in the fastest path, and vary the switching speed. This also leads to an average speed of about 50mph if driving along the fastest path. As in Figure 6, the reduced emission compared to PASO is very small when the switching speed is below 44mph, which is significantly smaller than the average speed. Hence, despite
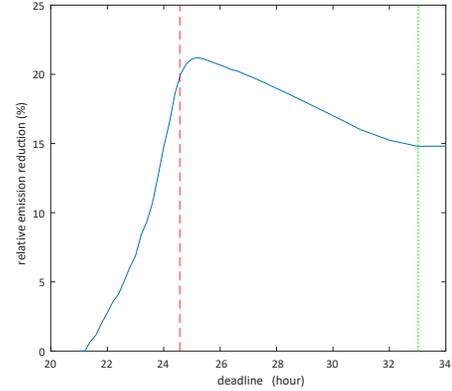
Figure 7: Reduced emission from MFI compared to PASO vs. deadline. The dashed line denotes the travel time driving at the switching speed (49mph) along the fastest path, and the dotted line is the travel time driving at the minimum speed (30mph) along the shortest path.

the existence of the triple-injection strategy that provides better emission, our approach is largely unable to leverage it and has to use the single-injection strategy most of the time. Hence, it does not reduce emission compared to PASO. However, when the switching speed goes up, the percentage of reduced emission rises quickly, to finally reach about 23%. In all cases, the emission from MFI is at least 1.5 times less than that of FAST, indicating the importance of speed planning for emission reduction.

We then study how the reduced emission varies with the deadline. We set the switching speed to be 49mph, and vary the deadline from 20 hours (1.10 times the travel time of FAST) to 26 hours (1.42 times the travel time of FAST). Figure 7 illustrates the relative emission reduction of MFI compared to PASO. As in the figure, when the deadline is relatively small (less than 21 hours), the truck is forced to drive in the speed range of the single injection strategy, hence providing no benefit compared to PASO. However, MFI can still provide substantial emission reduction, even if the deadline is significantly smaller than the total travel time of driving at the switching speed 49mph along the fastest path (denoted as dashed line in the figure), hence only allowing a portion of the edges to drive below the switching speed. The relative reduced emission after the dashed line mostly follows the relative gap between the emissions of single-injection and triple-injection strategies. It becomes smaller when the speed becomes smaller (hence with longer travel time), and saturates after the dotted line (the minimum travel time, i.e., driving at the minimum speed along the shortest path).

We now simulate over a large number of source-destination pairs, by randomly select a source region from the eastern US and another different region as the destination. We set the deadline for MFI and PASO as 1.33 times of the travel time of FAST, and fix the switching speed to be 49mph. For these instances, on average MFI saves about 72.2% of the emission compared to FAST, by selecting a path and speed profile that minimize the emission while still meeting the deadline. Compared to PASO, MFI reduces about 18.2% of the total emission, demonstrating our capability of leveraging adaptive injection strategy to operate trucks in a more environmental friendly fashion.

7 CONCLUSION

In this paper, we consider the scenario that a truck to haul freights across a national highway system within a given deadline. We ride on the recent advancement in engine control that adaptively selects the fuel injection strategy to effectively reduce the emission. We show that the problem is NP-complete, and the adaptive fuel injection strategy imposes a unique challenge compared to existing studies, as the emission rate function is non-continuous and non-convex. We leverage the special problem structure to derive an analytical solution to optimize speed profile. We then propose an efficient heuristic for the overall problem of path planning and speed planning, and derive a performance gap for the heuristic.

We evaluate our solutions using real-world traces over the US national highway system. Our solutions can save on average 18% emission compared to the baseline with a single control strategy. Compared to the fastest path approach that is adopted in common practice, our scheme reduces 72% emission on average. Our future work includes the consideration of dynamic traffic condition and multiple transportation tasks.

REFERENCES

[1] A. Alam, B. Besselink, V. Turri, J. Mårtensson, and K. Johansson. Heavy-duty vehicle platooning for sustainable freight transportation: A cooperative method to enhance safety and efficiency. *IEEE Control Syst. Magazine*, 35(6):34–56, 2015.
[2] A. Alam, J. Mårtensson, and K. Johansson. Look-ahead cruise control for heavy duty vehicle platooning. In *IEEE International Conference on Intelligent Transportation Systems*, 2013.
[3] A. Alam, J. Mårtensson, and K. Johansson. Experimental evaluation of decentralized cooperative cruise control for heavy-duty vehicle platooning. *Control Engineering Practice*, 38:11–25, 2015.
[4] American Trucking Associations. American Trucking Trends 2019. https://www.trucking.org/news-insights/ata-american-trucking-trends-2019.
[5] H. Ashby. *Protecting Perishable Foods during Transport by Truck*. U.S. Department of Agriculture, 2006.
[6] A. Biondi, M. D. Natale, G. C. Buttazzo, and P. Pazzaglia. Selecting the transition speeds of engine control tasks to optimize the performance. *ACM Transactions on Cyber-Physical Systems*, 2(1):1–26, 2018.
[7] K. Boriboonsomsin, M. Barth, W. Zhu, and A. Vu. Eco-routing navigation system based on multisource historical and real-time traffic information. *IEEE Transactions on Intelligent Transportation Systems*, 13(4):1694–1704, 2012.
[8] S. Boyd and L. Vandenberghe. *Convex optimization*. Cambridge univ. press, 2004.
[9] D. Buttle. Keynote speech: Real-time in the prime-time. In *Euromicro Conference on Real-Time Systems*, 2012.
[10] California Air Resources Board. California Air Resources Board staff current assessment of the technical feasibility of lower NOx standards-White paper. https://ww3.arb.ca.gov/msprog/hdlownox/white_paper_04182019a.pdf.
[11] California Air Resources Board. NOx Emissions of In-Use Trucks. https://ww2.arb.ca.gov/resources/documents/nox-emissions-of-in-use-trucks.
[12] L. Deng, M. H. Hajiesmaili, M. Chen, and H. Zeng. Energy-efficient timely transportation of long-haul heavy-duty trucks. In *7th International Conference on Future Energy Systems*. ACM, 2016.
[13] L. Deng, M. H. Hajiesmaili, M. Chen, and H. Zeng. Energy-efficient timely transportation of long-haul heavy-duty trucks. *IEEE Transactions on Intelligent Transportation Systems*, 19(7):2099–2113, 2018.
[14] R. Hassin. Approximation schemes for the restricted shortest path problem. *Mathematics of Operations research*, 17(1):36–42, 1992.
[15] E. Hellström, M. Ivarsson, J. Åslund, and L. Nielsen. Look-ahead control for heavy trucks to minimize trip time and fuel consumption. *Control Engineering Practice*, 17(2):245–254, 2009.
[16] Traffic flow using corridor in HERE maps. https://developer.here.com/api-explorer/rest/traffic/flow-using-corridor.
[17] Y. Hotta, M. Inayoshi, K. Nakakita, K. Fujiwara, and I. Sakata. Achieving lower exhaust emissions and better performance in an hsdi diesel engine with multiple injection. In *SAE Technical Paper*, 2005.
[18] M.-F. Hsieh and J. Wang. No and no2 concentration modeling and observer-based estimation across a diesel engine aftertreatment system. *Journal of Dynamic Systems, Measurement, and Control*, 133(4), 2011.
[19] International Energy Agency. *The Future of Trucks*. https://www.oecd-ilibrary.org/content/publication/9789264279452-en, 2017.
[20] T. Johnson and A. Joshi. Review of vehicle engine efficiency and emissions. *SAE International Journal of Engines*, 11(6):1307–1330, 2018.
[21] A. Juttner, B. Szviatovski, I. Mécs, and Z. Rajkó. Lagrange relaxation based method for the qos routing problem. In *IEEE Conf. Computer Communications*, 2001.
[22] Y. Kim, Y. Kim, S. Jun, K. Lee, S. Rew, D. Lee, and S. Park. Strategies for particle emissions reduction from gdi engines. In *SAE Technical Paper*, 2013.
[23] Q. Liu, H. Zeng, and M. Chen. Energy-efficient timely truck transportation for geographically-dispersed tasks. In *ACM Conf. Future Energy Systems*, 2018.
[24] Q. Liu, H. Zeng, and M. Chen. Energy-efficient timely truck transportation for geographically-dispersed tasks. *IEEE Transactions on Intelligent Transportation Systems*, pages 1–12, 2019.
[25] D. Lorenz and D. Raz. A simple efficient approximation scheme for the restricted shortest path problem. *Operations Research Letters*, 28(5):213–219, 2001.
[26] W. Mallett. *Freight Performance Measurement: Travel Time in Freight-Significant Corridors*. U.S. Federal Highway Administration, 2006.
[27] C. Peng, Y. Zhao, and H. Zeng. Dynamic switching speed reconfiguration for engine performance optimization. In *56th Design Automation Conference*, 2019.
[28] R. Rajput. *A text book of automobile engineering*. Firewall Media, 2008.
[29] P. Sahlholm and K. H. Johansson. Road grade estimation for look-ahead vehicle control using multiple measurement runs. *Control Engineering Practice*, 18(11):1328–1341, 2010.
[30] G. Scora, K. Boriboonsomsin, and M. Barth. Value of eco-friendly route choice for heavy-duty trucks. *Research in Transportation Economics*, 52:3–14, 2015.
[31] J. Su, M. Xu, P. Yin, Y. Gao, and D. Hung. Particle number emissions reduction using multiple injection strategies in a boosted spark-ignition direct-injection (sidi) gasoline engine. *SAE International Journal of Engines*, 8(1):20–29, 2015.
[32] J. Teresco. Map-based Educational Tools for Algorithm Learning (METAL) project. https://courses.teresco.org/metal/.
[33] United States Environmental Protection Agency. Greenhouse Gases Equivalencies Calculator. https://www.epa.gov/energy/greenhouse-gases-equivalencies-calculator-calculations-and-references.
[34] USGS Elevation Point Query Service. http://nationalmap.gov/epqs/.
[35] Wikipedia. Convex function. https://en.wikipedia.org/wiki/Convex_function.
[36] Wikipedia. Semi-differentiability. https://en.wikipedia.org/wiki/Semi-differentiability.
[37] W. Xu, Q. Liu, M. Chen, and H. Zeng. Ride the tide of traffic conditions: Opportunistic driving improves energy efficiency of timely truck transportation. In *ACM Conf. Systems for Energy-Efficient Buildings, Cities, and Transportation*, 2019.

8 APPENDIX

8.1 Proof of Lemma 4

We first restate a useful lemma for univariate convex functions [35].

LEMMA 11. *[35] Suppose $g(x)$ is a function of one real variable x. Consider the slope $S(x_1, x_2) = \frac{g(x_2) - g(x_1)}{x_2 - x_1}$ of the line connecting two points $(x_1, g(x_1))$ and $(x_2, g(x_2))$ on the curve. g is convex if and only if $S(x_1, x_2)$ is monotonically non-decreasing in x_1, for every fixed x_2.*

Now we prove the lemma.

PROOF (OF LEMMA 4). For any given x_1, it is easy to see that β is uniquely determined as $\beta = \frac{\bar{x} - x_1}{x_2 - x_1}$. Hence,

$$\bar{y} = \frac{x_2 - \bar{x}}{x_2 - x_1} y_1 + \frac{\bar{x} - x_1}{x_2 - x_1} y_2$$
$$= y_2 + \frac{g(x_2) - g(x_1)}{x_2 - x_1}(\bar{x} - x_2) + \frac{(x_2 - \bar{x})(y_2 - g(x_2))}{x_1 - x_2}$$

By Lemma 11 and that $(\bar{x} - x_2)$ is non-positive, the second summand on the right hand side is monotonically non-increasing with x_1. The third summand is also monotonically non-increasing with x_1, since both $(x_2 - \bar{x})$ and $(y_2 - g(x_2))$ are non-negative. Hence, $\bar{y}$ is also monotonically non-increasing with x_1. □

8.2 Proof of Lemma 5

We first consider a lemma similar to Lemma 11, which concerns the slope connecting a point below the curve of a convex function and any point on the curve but to the right of the first point.

Lemma 12. *Suppose $g(x)$ is a convex function of one real variable x. For a point (x_1, y_1) that is below $g(x)$ (i.e., $y_1 < g(x_1)$), the slope of the line connecting (x_1, y_1) to any point $(x_2, g(x_2))$ on the right (i.e., $x_1 < x_2$) is first monotonically non-increasing with x_2 before p, then monotonically non-decreasing with x_2 after p, where $p > x_1$ is the generalized right point of tangency from (x_1, y_1) to the curve $g(x)$.*

Proof. The slope of the line connecting (x_1, y_1) and $(x_2, g(x_2))$ is $T(x_2) = \frac{g(x_2) - y_1}{x_2 - x_1}$. Consider two values b and a for x_2 such that $b \geq a > x_1$.

Case 1: $a \leq b \leq p$. In this case, it is

$$T(a) = \frac{g(a) - y_1}{a - x_1} \overset{(I1)}{\geq} \frac{g(b) + \partial_- g(b)(a - b) - y_1}{b - x_1}$$
$$\overset{(I2)}{\geq} \frac{g(b) + \frac{g(b) - y_1}{b - x_1}(a - b) - y_1}{a - x_1} = \frac{g(b) - y_1}{b - x_1} = T(b)$$

Here inequality $(I1)$ is because g is convex hence $g(a) - g(b) \geq \partial_- g(b)(a - b)$, and inequality $(I2)$ is because b is no larger than the generalized right point of tangency p.

Case 2: $b \geq a \geq p$. In this case, we have

$$T(b) = \frac{g(b) - y_1}{b - x_1} \overset{(I3)}{\geq} \frac{g(a) + \partial_+ g(a)(b - a) - y_1}{b - x_1}$$
$$\overset{(I4)}{\geq} \frac{g(a) + \frac{g(a) - y_1}{a - x_1}(b - a) - y_1}{b - x_1} = \frac{g(a) - y_1}{a - x_1} = T(a)$$

Here inequality $(I3)$ is because g is convex hence $g(b) - g(a) \geq \partial_+ g(a)(b - a)$, and inequality $(I4)$ is because a is no smaller than the generalized right point of tangency p. □

We now proceed to prove Lemma 5.

Proof of Lemma 5. It is easy to see that $\beta = \frac{\bar{x} - x_1}{x_2 - x_1}$. Hence,

$$\bar{y} = \frac{x_2 - \bar{x}}{x_2 - x_1} y_1 + \frac{\bar{x} - x_1}{x_2 - x_1} y_2 = y_1 + \frac{g(x_2) - y_1}{x_2 - x_1}(\bar{x} - x_1)$$

By Lemma 12 and that $(\bar{x} - x_1)$ is non-negative, the monotonicity of the second summand in the above equation and hence of $\bar{y}$ follows that of $T(x_2)$: monotonically non-increasing before p, then monotonically non-decreasing after p.

If $\bar{x} \leq p$, since $\bar{y}$ is monotonically non-increasing with $x_2, \forall x_2 \in [\bar{x}, p]$, we have

$$\bar{y} = y_1 + \frac{g(x_2) - y_1}{x_2 - x_1}(\bar{x} - x_1) \leq y_1 + \frac{g(\bar{x}) - y_1}{\bar{x} - x_1}(\bar{x} - x_1) = g(\bar{x})$$

If $\bar{x} \geq p$, since $\bar{y}$ is monotonically non-decreasing with $x_2, \forall x_2 \geq \bar{x} \geq p$, we have

$$\bar{y} = y_1 + \frac{g(x_2) - y_1}{x_2 - x_1}(\bar{x} - x_1) \geq y_1 + \frac{g(\bar{x}) - y_1}{\bar{x} - x_1}(\bar{x} - x_1) = g(\bar{x})$$

□

8.3 Proof of Theorem 6

Proof by induction.

Base case $n = 1$. This is straightforward since the only feasible (and thus also optimal) solution to problem (5) is $r_1 = \bar{r}, \beta_1 = 1$. This is consistent with Equation (12) where it is described by Case 1. Hence $f^*(\bar{r}) = f_1(\bar{r})$, which is obviously convex too.

Induction Step. Assume the theorem holds for $n = k$. Now consider an arbitrary emission rate function $f(r)$ containing $n =$

$k + 1$ pieces, we define a new function $\hat{f}(r)$ containing k pieces, as defined in Equation (6). By the inductive assumption, $\hat{f}^*(r)$ is convex. In addition, by the assumption in Equation (2) and the fact that $\hat{f}^*(r)$ is a convex combination of $f_1(r), ..., f_k(r)$, it must be that

$$\hat{f}^*(r) < f_{k+1}(r), \forall r \tag{20}$$

By Equation (8), the problem of finding f^* for a given $\bar{r}$ is essentially to find a point $(\hat{r}, \hat{f}^*(\hat{r}))$ on the convex curve $\hat{f}^*$ and another one $(r_{k+1}, f_{k+1}(r_{k+1}))$ on the curve f_{k+1} such that the speed of the convex combination is $\bar{r}$, and the cost is minimized. By Equation (20) and that $\hat{r} < r_{k+1}$, Lemma 4 and Lemma 5 are both applicable. Note that it must be $\hat{r} \leq \bar{r}$ since $r_{k+1} > \hat{r}$.

Case 1: $\bar{r} \in (s_0, s_k]$. In this case, by Lemma 4, $\hat{r} = \bar{r}$, and the optimal cost to problem (8) is always no smaller than $\hat{f}^*(\bar{r})$. On the other hand, the solution $\hat{r} = \bar{r}, \beta_{k+1} = 0$ achieves a cost equal to $\hat{f}^*(\bar{r})$, hence it must be an optimal solution to problem (8). This solution essentially is to use only the first k pieces in $f(\cdot)$, which follows the optimal solution in $\hat{f}^*(\bar{r})$, and by recursion goes to the i-th piece that $\bar{r}$ sits in.

Case 2: $\bar{r} \in (s_k, s_{k+1}]$. By Lemma 4, $\hat{r} = s_k$, which implies that $r_k = s_k$ and $\beta_j = 0, \forall j < k$.

By Lemma 5, the optimal solution to problem (8) follows that of the Case 2 or Case 3 in Equation (12), for which $i = k + 1$. Specifically, if $\bar{r} \leq p_{k+1}$, then since $\hat{f}^*(\bar{r})$ is monotonically non-increasing before p_{k+1} and non-decreasing afterwards, the optimal assignment to r_{k+1} is the maximum value before reaching p_{k+1}, i.e., $\min(p_{k+1}, s_{k+1})$. If $\bar{r} \geq p_{k+1}$, the optimal assignment to r_{k+1} is its lower bound $\bar{r}$, which implies $\beta_k = 0$ and $\beta_{k+1} = 1$.

We now prove the convexity of $f^*(\bar{r})$. As above, $f^*(\bar{r})$ contains two parts, the first is that of Case 1 where $f^*(\bar{r}) = \hat{f}^*(\bar{r})$, the second is that of Case 2, and the breakpoint is s_k. Within the part of Case 2, there might also exist two pieces: it contains a linear segment connecting $(s_k, \hat{f}^*(s_k))$ to $(r_{k+1}, f_{k+1}(r_{k+1}))$ where $r_{k+1} = \min\{p_{k+1}, s_{k+1}\}$, and a possible second segment using f_{k+1} if $p_{k+1} < s_{k+1}$. We only need to prove that the left derivative $\partial_- f^*$ is no larger than the right derivative $\partial_+ f^*$ at both these breakpoints s_k and p_{k+1}, since f^* is convex within each piece.

At the breakpoint s_k, we have

$$\partial_+ f^*(s_k) = \frac{f_{k+1}(r_{k+1}) - \hat{f}^*(s_k)}{r_{k+1} - s_k} \overset{(I5)}{\geq} \frac{\hat{f}^*(r_{k+1}) - \hat{f}^*(s_k)}{r_{k+1} - s_k}$$
$$\overset{(I6)}{\geq} \partial_+ \hat{f}^*(s_k) \overset{(I7)}{\geq} \partial_- \hat{f}^*(s_k) = \partial_- f^*(s_k)$$

Here inequality $(I5)$ is from Equation (20). Inequalities $(I6)$ is because of the inductive assumption that $\hat{f}^*$ is convex, hence its curve lies above the right tangent at s_k. Likewise, $(I7)$ holds because the left derivative of the convex function $\hat{f}^*$ is no larger than its right derivative at any point, in particular s_k.

At the breakpoint p_{k+1} (which only exists if $p_{k+1} < s_{k+1}$), it is

$$\partial_- f^*(p_{k+1}) = \frac{f_{k+1}(p_{k+1}) - \hat{f}^*(s_k)}{p_{k+1} - s_k}$$
$$\overset{(I8)}{\leq} \partial_+ f_{k+1}(p_{k+1}) = \partial_+ f^*(p_{k+1})$$

Here inequality $(I8)$ holds because $(p_{k+1}, f_{k+1}(p_{k+1}))$ is the generalized right point of tangency from $(s_k, \hat{f}^*(s_k))$ to the curve f_{k+1}.